Journal of the European Ceramic Society 19 (1999) 2883–2891

PII: S0955-2219(99)00054-0
0955-2219/99/$ - see front matter

Rheological Analysis of Ceramic Pastes

Necati Özkan, [a] Cüneyt Oysu, [b] Brian J. Briscoe [c] * and Ismail Aydin [c]

[a]Department of Chemical and Materials Engineering, University of Auckland, Auckland, New Zealand
[b]Department of Mechanical Engineering, Imperial College, London SW7 2BY, UK
[c]Department of Chemical Engineering, Imperial College, London SW7 2BY, UK

(Received 12 October 1998; accepted 21 February 1999)

Abstract

This paper is concerned with a number of means of characterising the rheological properties of a ceramic paste. The intrinsic flow behaviour of the paste, during upsetting, is studied experimentally by using multi coloured paste samples, as well as by a finite element numerical computation. The flow behaviour of the paste is approximated by an elasto-viscoplastic material constitutive model and implemented by using an established finite element code. The material flow properties, which are necessary for the implementation of the numerical model, were obtained using the squeeze film and hardness indentation test configurations. The flow fields generated by the simulation are shown to be a good accord with the experimental observations. The experimental procedure for selecting the material parameters which are necessary for the implementation of the numerical model is described. The accuracy of the numerical method described is also evaluated by comparing the simulation results with experimental data obtained from the net upsetting force against the imposed relative displacement behaviour and the flow visualisation of deformed coloured layers. In these respects, a comparison of the finite element model predictions and the experimental results demonstrates a good mutual agreement. © *1999 Elsevier Science Ltd. All rights reserved*

Keywords: shaping, plastic forming, elasto-viscoplasticity, finite element analysis.

1 Introduction

Paste materials are encountered in a wide range of industries, either as an intermediary or as the final product, including food, pharmaceutical, and ceramic products. Ceramic manufacturing by extrusion, injection moulding, and tape rolling (calendering) requires a suitable plastic precursor which is often called a 'paste'. The common feature of these forming techniques is that a desirable shape is formed from a mixture of powders and additives that provides a coherent and extensively deformable plastic mass which also has some capacity to retain its given shape. Organic materials (binders and plasticisers) are added with a suitable solvent to provide the necessary plasticity and elasticity.

The parameters such as the load, the stress, and the strain distributions depend upon the bulk flow properties of the paste and also upon the wall boundary condition between the paste and the rigid walls of the processing equipment. These pastes are elasto-viscoplastic materials and they exhibit relatively complex flow and wall boundary properties. The main characteristic of paste processing is the application of relatively large strains, or material displacements, by the imposition of stresses transmitted via rigid walls. Computer simulation techniques may provide useful information for determining the process parameters and hence help to optimise the manufacturing process of these materials. Process simulation has been a major recent concern in paste forming technology for the enabling of the proper design and control which requires the determination of the deformation mechanics involved. The effects of various processing parameters on the details of the paste flow during processing are not easy to investigate because of the complicated interactions which develop between the wall boundary and the intrinsic rheology of the material. Particulate paste materials behave, to a good approximation, as viscoplastic fluids[1,2] where complex bulk flow and interfacial properties are exhibited. Accurate determination of the deformation mechanics is potentially possible when the finite element method is applied to the analysis of paste forming processes. To examine the validity of such numerical techniques, it is desirable to investigate

* To whom correspondence should be addressed. Fax: +44-171-5945561; e-mail: b.briscoe@ic.ac.uk

and establish the bulk and interfacial flow behaviour in nominally simple flows such as the squeeze film[2] and upsetting configurations.[3–6]

The current paper describes an investigation of the application of a numerical simulation method to the upsetting of an alumina paste and a comparison of these results with selected experimental data. The aim is to develop a data analysis procedure for determining intrinsic material deformation parameters and wall boundary characteristics for ceramic pastes which may also be used for other forming operations as well as for the design of processing equipment. The bulk flow constitutive relationship was modelled by an elasto-viscoplastic equation and the reaction load, stress and strain distributions were computed at each stage of the deformation. The material flow parameters were obtained using various experimental procedures; the squeeze film method, the hardness indentation procedure, and by the upsetting of cylindrical alumina paste samples. For the interpretation of the experimental data, the viscoplastic Herschel–Bulkley model was adopted. The numerical results are compared with various experimental data obtained in the upsetting of the alumina paste.

2 Experimental

2.1 Paste preparation

A commercial alumina (AES-11, Morgan Matroc, UK) with an average particle size of 0·4 μm was combined with methyl-ethyl-ketone (MEK) (solvent, Aldrich Chemicals Co., UK), poly (vinyl butyral) (PVB) (dispersant and binder, Aldrich Chemicals Co., UK) and dibuthyl phthalate (DBP) (plasticiser, Aldrich Chemicals Co., UK) to produce the paste system. Initially, the dispersant was mixed with the solvent in a glass beaker, and then the alumina powder was added to the solvent mixture. In order to attempt to breakdown the agglomerates, the suspension was ultrasonicated for 3 min using a Vibra-Cell (model CV26) ultrasonicater and subsequently ball milled for 12 h. After adding the binder and plasticiser, the suspension was ball-milled for a further 24 h in order to obtain a well dispersed suspension. The ceramic paste was obtained by removing the solvent from the suspension under the action of continuous stirring in a water bath at 60°C. All the samples were then allowed to equilibrate to 21°C for 24 h in a temperature controlled laboratory prior to examination. At the end of the sample preparation, a stable paste system was obtained without any solvent content.

2.2 Squeeze film and upsetting tests

For the squeeze film and upsetting tests, cylindrical specimens were cut from sheets of the alumina paste specimens, with various thickness values, prepared using the roll milling technique.[7] The thickness of the alumina pastes was fixed by adjusting the gap between the rolls. Especially fabricated cutters were used for the cutting of cylindrical samples of the required dimensions. The dimensions (initial diameter: initial height) chosen for the squeeze film and upsetting tests were 22·00:3·37 mm and 22·0:22·0 mm, respectively. Two parallel platens were used for the uniaxial compression of the cylindrical specimens. These platens were attached to the cross heads of a commercial universal testing machine (Instron 1120, UK). The reaction load was recorded by a load cell and the displacement was obtained from an LVDT attached externally to the cross-head. The experimental arrangements for these test configurations are illustrated in Fig. 1. In order to create a wall boundary condition with high wall friction coefficient, conventional Emery Papers (400 grade) were inserted between the platens and the ceramic paste specimens. For the 'lubricated' interface case, a commercial silicone grease was interposed at the interface between the ceramic paste material and the platen surfaces.

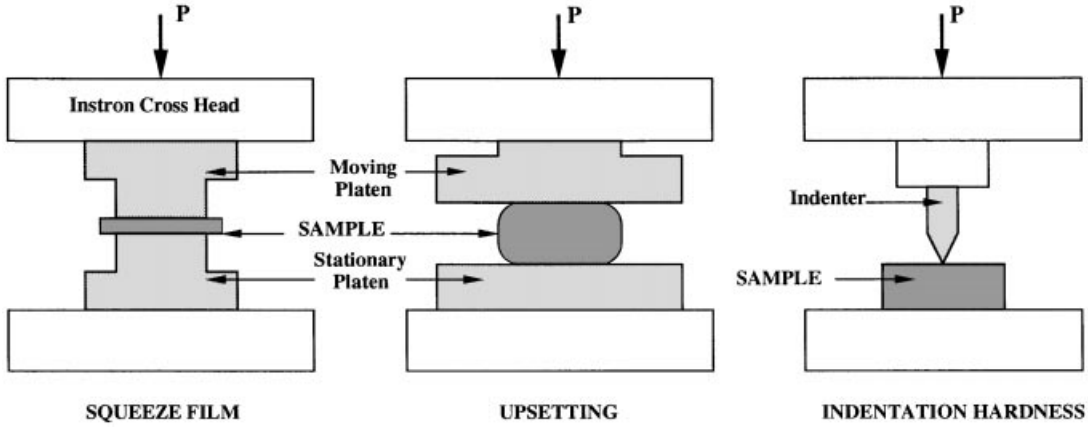

Fig. 1. Experimental test configurations.

The flow visualisation of the paste deformation process, during the upsetting test, was achieved by using the coloured alumina pastes (green and red) which were used to produce cylindrical paste samples containing various layers (thickness = 3·37 mm and diameter = 22·00 mm) of the alternating colours. These samples were then compressed between parallel platens. After the compression test, the samples with the alternating layers were cut into halves with a plane passing through the major axis of the samples for the purpose of the photography in order to observe the flow patterns of the samples.

2.3 Hardness indentation test

A standard universal testing machine (Instron 1122, UK) was adapted for the hardness indentation tests, taking advantage of the load sensors and actuator systems available in the machine; Fig. 1. A separate LVDT (Schlumberger, UK) was used in order to record the imposed displacement. The indenter, a steel cone (90° induced angle) was fixed in a special holder attached to the crosshead of the testing machine. The specimen was supported upon an alignment platform attached to the load cell.

3 Experimental Results

We have used three experimental compressive deformation fields which are summarised in Table 1; the response of all three depends upon the prevailing boundary conditions. There are first order models of various quality for describing all three. Response is geometry, boundary condition, and rheology dependent.

The experimental results, obtained from the hardness indentation test, the squeeze film, and the upsetting configurations, were analysed in order to obtain the plastic and viscous properties of the paste. Table 2 summaries the choices of the rheological relationships which have been adopted in these analyses.

3.1 Squeeze film

A number of analytical analyses have been developed for the interpretation of the results obtained from the squeeze film configuration. Here, the 'Scott Analysis'[8] has been adopted. For a power law liquid (as in eqn. (2), described later), Scott obtained the following equation:

$$F = \frac{2\pi k\left(-\dot{h}\right)^n R^{n+3}}{h^{2n+1}(n+3)}\left(\frac{2n+1}{n}\right)^n \tag{1}$$

where F is the squeeze force, k is the flow consistency, h is the height of the specimen, $\dot{h}$ is the platen velocity, R is the radius of the specimen, and n is the flow index.

In the squeeze film test, the alumina paste in the form of a cylindrical disc is compressed between two parallel steel platens. The effective radius of the specimen is kept constant by maintaining the radius of the alumina paste sample larger than that of the rigid circular platens. Therefore, the material outside the platen contact zone does not significantly contribute to the total squeeze force during the test. The squeeze force as a function of the 'film' height for various platen velocities is illustrated in Fig. 2. As can be seen from Fig. 2, the squeeze force increases as the film height decreases.

Table 1. The experimental configurations used in this study

	Deformation	*Contact area*	*Deformation volume*	*Fields*
Squeeze film	Homogeneous[a]	Fixed	Varies	Non-homogeneous
Upsetting	Homogeneous[a]	Varies	Fixed	Non-homogeneous
Hardness	Local	Varies	Varies[b]	Non-homogeneous

[a] Nominal.
[b] Perhaps.

Table 2. The results for the alumina paste

Relationship	*Techniques*	*Form of equation*	*Parameters*		
			σ_o *(MPa)*	n	k
Power law	Squeeze film	$\tau = k(\dot{\gamma})^n$	—	0·35	1·61
		$\sigma = k_a\dot{\varepsilon}^n$	—	0·35	3·38
	Hardness	$\tau = k(\dot{\gamma})^n$	—	0·31	0·26
		$\sigma = k_a\dot{\varepsilon}^n$	—	0·31	0·54
Hersched–Bulkley	Squeeze film	$\tau = \tau_o + k(\dot{\gamma})^n$	0·058	0·363	1·544
		$\sigma = \sigma_o + k_a(\dot{\varepsilon})^n$	0·10	0·363	3·26

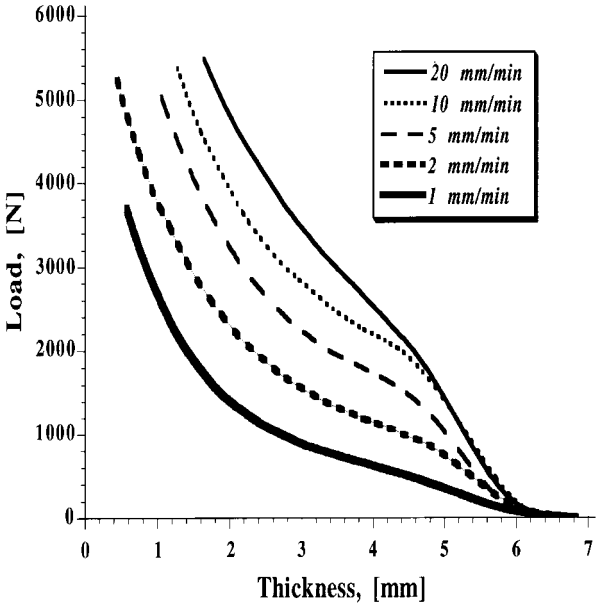

Fig. 2. The squeeze force as a function of the film thickness for various platen velocities.

The platen velocity also has strong effect upon the squeeze force; the higher the platen velocity the larger the squeeze force. Using eqn. (1), the n and k values for the alumina paste system were calculated from the slope and intercept of the plot of $\ln(F)$ against $\ln(h)$ as in the units of (N) and (m/s), respectively.

For a power law model of the form:

$$\tau = k_s\left(\dot{\gamma}^{\mathrm{pl}}\right)^{n_1} \tag{2}$$

where τ and $\dot{\gamma}^{\mathrm{pl}}$ represent the shear stress and the plastic shear strain rate, the flow parameters; shear plastic flow consistency, k_s, and flow index, n_1, are obtained as 1·61 MPa and 0·354, respectively.

3.2 Upsetting

A first order analysis for the upsetting of a rigid–plastic cylindrical specimen, of radius R and current thickness h, was first proposed by Siebel. According to this analysis, the mean compressive wall stress, p_m, is given as follows:[9]

$$P_m = \sigma_o + \frac{2}{3}\sigma_o\mu\left(\frac{R}{h}\right)$$

The yield stress of the paste (σ_o) and wall friction coefficient (μ) may be calculated from the intercept and the slope of the plot of p_m against (R/h). The yield stress for the alumina paste was calculated as 0·186 and 0·0117 MPa for the platen approach speeds of 10 and 1 mm min^{-1}, respectively, and the friction coefficient was calculated as 2·77 and 18·8 for the plated speed of 10 and 1 mm min^{-1}, respectively. The calculated friction coefficients obtained using this analysis are invariably unrealistic. These results clearly indicate that this simple first order analysis is not suitable. This analysis can only predict the flow parameters when the material obeys the laws of plasticity and its response is not dependent upon the imposed strain or the strain rate. However, it was shown that the response of the alumina paste is different under the conditions of varying the strain and the strain rates. In addition, this type of analysis assumes a true homogeneous deformation of the material within the bulk. Therefore, this analysis should not be used to obtain the material parameters for the materials whose response depends upon the strain and strain rates.

The upsetting configuration was used to investigate the nonhomogeneous flow by visualisation of the deformation of alumina pastes. The experimental results, obtained using the upsetting configurations, will be reported together with FEA simulation results in Section 5.

3.3 Indentation hardness test

The indentation hardness test was used to obtain the hardness (a plastic yield characteristic) and the elastic modulus of the ceramic pastes. In order to compute these material properties a contact compliance procedure, in conjunction with an analysis based upon an adaptation of the Box–Cox curve fitting method for the compliance curve, was used.[10,11] A hardness compliance curve obtained for the alumina paste is illustrated in Fig. 3. The hardness and reduced elastic modulus values of this paste system were calculated as 0·25 and 4·5 MPa, respectively. The relationship between the hardness (H) or approximately the mean contact pressure (σ_c) and the yield stress (σ_o) is conventionally assumed to be of the following form for materials where the ratio of $(\sigma_o/E)\cot\phi$ (where ϕ is the semi-complement of the conical indenter) which is greater than some minimum value.[12]

$$H = \sigma_c = B\sigma_o \tag{3}$$

where B is a dimensionless factor whose value is a function of at least the material response character (the relative elastic/plastic behaviour), the contact strain, and the interface friction.[13] The value of B is generally found in the ranges from ca 1·5 to 3. For a fully plastic response B is near 3 and for the cases where a significant elastic contribution is evident B is nearer to the lower limit. In the case of a fully elastic material the relationship is naturally not applicable. The plastic yield stress of the ceramic paste was calculated as 0·1 MPa assuming B is equal to 2·5 and using eqn. (3). The elastic modulus of the ceramic paste is calculated as ca 4·0 MPa using the following equation

$$E^* = \frac{E}{1-\upsilon^2} \tag{4}$$

where E^* is the reduced elastic modulus, E is the elastic modulus, and υ is the Poisson's ratio. The value of Poisson's ratio was selected as 0·33 since the best agreement between the experimental and predicted deformed patterns was obtained using this value. These results are reported in Section 5.

A power-law creep model, which was initially described by Mulhern and Tabor and may be used to describe time-dependent indentation, is given as

$$\sigma = k_a \dot{\varepsilon}^{n_3} \tag{5}$$

where σ is the uniaxial flow stress, k_a is the uniaxial flow consistency, n_3 is the flow index, and $\dot{\varepsilon}$ is the strain rate. When we assume that the yield stress in eqn. (3) may be substituted by the flow stress in eqn. (5), we obtain the following relationship:

$$\sigma_c = Bk_a\dot{\varepsilon}_{eff})n_3 \tag{6}$$

where $\dot{\varepsilon}_{eff}$ is an effective strain rate which would be experienced in a simple tensile or compression test and is approximately equal to $\dot{h}/h\tan\phi$ where $\dot{h}$ and h are the imposed penetration velocity and depth, respectively.[14] In order to obtain the parameters k_a and n_3 for the constitutive equation [eqn. (6)], the compliance curves for various penetration velocities were obtained. The Bk_a and n_3 values of the alumina paste were calculated from the intercept and slope of the plot of ln (σ_c) against ln ($\dot{\varepsilon}_{eff}$) as 1·35 MPa and 0·31, respectively.

3.4 Interpretation of the results

The form of the power law model [eqn. (2)] may be converted into a Herschel–Bulkley Model form which is given as:

$$\tau = \tau_o + k_{s1}\left(\dot{\gamma}^{\mathrm{pl}}\right)^{n_2} \tag{7}$$

The value of the limiting shear yield stress, τ_o, may be calculated as ca 0·058 MPa obtained from the hardness indentation results for a von Mises yield criterion. By selecting 'k_{s1}' and 'n_3' values for the Herschel–Bulkley Model as 1·544 and 0·363, respectively, the power law model was translated into the Herschel–Bulkley Model. The computed flow curves, for the Power law and Herschel–Bulkley models, are illustrated in Fig. 4. Upon inserting the numerical values to the Herschel–Bulkley equation [eqn. (7)], the following interrelationship is obtained

$$\tau = 0{\cdot}058 + 1{\cdot}544\left(\dot{\gamma}^{\mathrm{pl}}\right)^{0{\cdot}363} \tag{8}$$

As may be seen from Fig. 4, when the yield stress value of the material is relatively low a power law equation [eqn. (2)] is successfully transformed into a Herschel–Bulkley equation [eqn. (8)].

The shear stress form of the Herschel–Bulkley relationship [eqn. (8)] may also be transformed to its uniaxial form. For a material that obeys the von Mises yield criterion, the uniaxial form of the Herschel–Bulkley relationship may be obtained from the shear stress-shear strain interrelationship. The uniaxial form of the corresponding Herschel–Bulkley is:

$$\sigma = \sigma_o + k_{a1}\left(\dot{\varepsilon}^{\mathrm{pl}}\right)^{n_4} \tag{9}$$

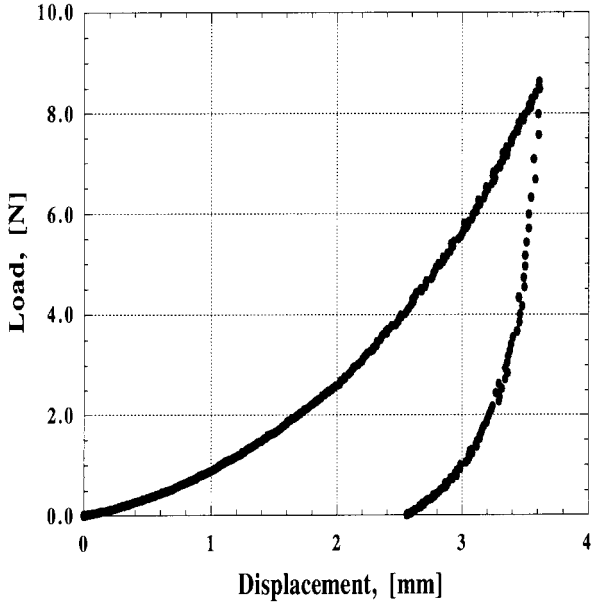

Fig. 3. The hardness compliance curve for the alumina paste.

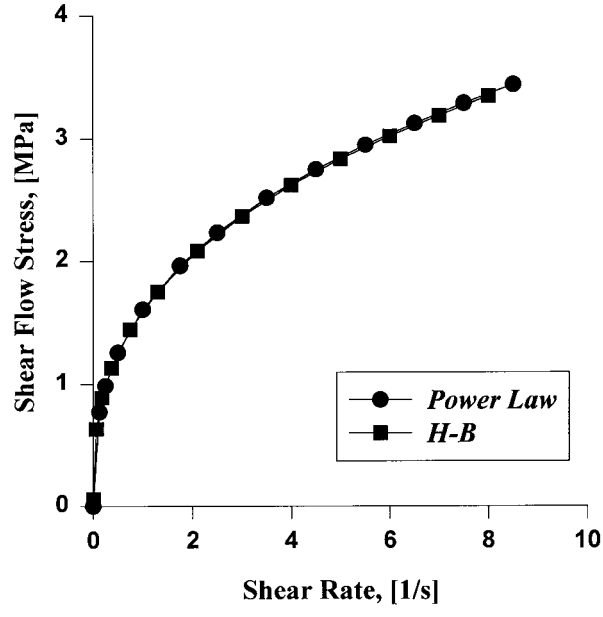

Fig. 4. The flow curves for the Power Law and Herschel–Bulkley models.

where σ_o is the static equivalent yield stress, k_{a1} and n_4 are the plastic flow consistency and the flow index, respectively. The interrelationships between the parameters in eqns (7) and (9) are as follows:

$$\sigma_o = \sqrt{3}\tau_o \tag{10}$$

and

$$k_{a1} = k_{s1}\left(\sqrt{3}\right)^{1+n_2} \tag{11}$$

By inserting the corresponding numerical values from eqn. (8), calculated by using eqns (10) and (11), eqn. (9) becomes:

$$\sigma = 0{\cdot}1 + 3{\cdot}26\left(\dot{\varepsilon}^{\mathrm{pl}}\right)^{0{\cdot}363} \tag{12}$$

Thus, a sufficient description of the elastic, plastic and viscous properties of the alumina paste is provided using the results obtained from the squeeze film and the indentation hardness tests.

The results obtained from the squeeze film and the hardness indentation results are summarised in Table 2. As may be seen from Table 2, there is a considerable difference between the values of k obtained using the squeeze film and the hardness indentation tests with the associated analyses. A possible explanation for this disagreement may be attributed to the definition of the effective strain rates for the two different geometries (the squeeze film and hardness indentation).

The k and n parameters of the ceramic paste obtained from the squeeze film analysis were used for the FEA simulation of the upsetting configuration since the definition of the effective strain rate for these geometries is the same. The σ_o and E values for the ceramic paste obtained from the hardness indentation test analysis were used for the FEA simulation for the upsetting configuration.

4 Finite Element Analysis

The finite element analysis for upsetting of the paste material was implemented by using the finite element code ABAQUS (Hibbitt, Karlsson and Sorensen, Inc., version 5.4). The details of analysis are given below.

4.1 Description of constitutive model and selection of material parameters

An elasto-viscoplastic model, provided within the material response library of the finite element code ABAQUS, was selected for the description of the flow behaviour of the paste material. The essential components of the model are described below:

i. The total strain is decomposed into elastic and plastic components so that the total strain rate, $\dot{\varepsilon}$, can be expressed as:

$$\dot{\varepsilon} = \dot{\varepsilon}^{\mathrm{el}} + \dot{\varepsilon}^{\mathrm{pl}} \tag{13}$$

where $\dot{\varepsilon}^{\mathrm{el}}$ and $\dot{\varepsilon}^{\mathrm{pl}}$ represent the equivalent elastic and plastic strain rates, respectively.

ii. The elastic response is treated as being linear. A constant Young's modulus of 4·5 MPa and a constant Poisson's ratio of 0·33 were incorporated.

iii. Strain rate dependence has been considered through:

$$\dot{\varepsilon}^{\mathrm{pl}} = D\left(\frac{\sigma}{\sigma_o} - 1\right)^p \text{ for } \sigma \leqslant \sigma_o \tag{14}$$

where σ is the equivalent yield stress at a nonzero strain rate, σ_o is the static equivalent yield stress, D and p are material parameters that contain the flow consistency and flow index, respectively (see below). The material parameters and were calculated by the following procedure.

The static equivalent yield stress, σ_o, value is obtained as 0·1 MPa. Equation (14) may be written in the form of eqn. (9) as:

$$\sigma = \sigma_o + \left(\frac{\sigma_o}{D1/p}\right)\left(\dot{\varepsilon}^{\mathrm{pl}}\right)^{1/p} \tag{15}$$

where $p = 1/n$ and $D = (\sigma_o/k)^p$. Therefore, the material parameters p and D are obtained as 2·755 and $6{\cdot}78\times10^{-5}$, respectively.

4.2 Geometry and boundary conditions

The geometry of the specimen is shown in Fig. 5. Due to the axisymmetric nature of the upsetting

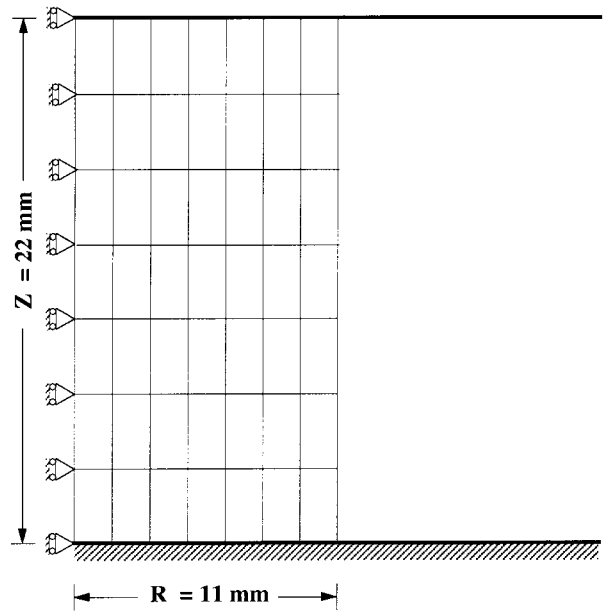

Fig. 5. The geometry of the specimen and the initial mesh used to implement the finite element analysis.

process, only half of the billet was modelled using a set of four-node axisymmetric continuum elements. The platens were modelled as rigid surfaces and interface elements were attached to the outer surface of the sample because of the expectation of a folding of the outer surface onto the platens. A Coulombic friction coefficient, μ, was assumed to be a constant wherever the paste billet contacts the platens. The axial displacement of the upper platen was prescribed as having a constant velocity (0·083 mm^{-1} s) in the axial direction. Mesh has been selected in a way that comparison of the flow fields can be made with the experimental data. No mesh convergence studies have been undertaken. The mesh used to initiate the analysis is shown in Fig. 5.

5 Numerical results and a comparison with the experimental data

The total upsetting response as a function of the imposed displacement of the upper die was also obtained using FEA with the associated material properties of the alumina paste ($E=4.0$ MPa, $\sigma_y=0{\cdot}1$ MPa, $\mu=0{\cdot}3$ (for the 'unlubricated' interface condition), and $\upsilon=0{\cdot}33$). The computed total upsetting force against the imposed displacement of the upper die with corresponding experimental data for the 'unlubricated' wall boundary condition is illustrated in Fig. 6. As may be seen from Fig. 6, an increasing force is required for the production of further deformation as the displacement is increased since the contact area increases during compression and the alumina paste material is a strain hardening material.

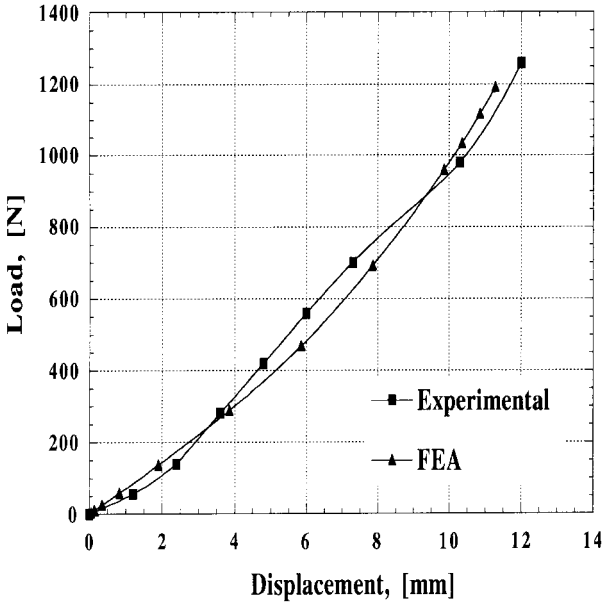

Fig. 6. The total upsetting force against the imposed displacement.

The computed distributions of the plastic equivalent strain, the axial stress, the hydrostatic pressure and the Mises stress during upsetting, at 50·0% (nominal strain) upsetting, are shown in Fig. 7 for the 'unlubricated' interface boundary condition. For this boundary condition, the static zones formed at the ends of the cylindrical specimen act like wedges and the specimen deforms by a process of 'folding' and 'barrelling'. As may be seen from these figures, the plastic deformation increases along the upper and lower platens. This process may also be observed from the increase of the angles of the elements, attached to the platens, towards the edge where the paste material is not free to move. As a result, the material on the side of the cylinder, adjacent to platens, folds onto the platens as the cylinder is compressed. This process is usually referred as 'folding'. On the other hand, the material near about a horizontal line, midway between the platens, is free to move in the radial direction. As a result, an increase in the diameter of the central region, compared with the interface regions, proceeds during upsetting; the process is referred as 'barrelling'. The high axial and hydrostatic stresses remain in the centre of the cylindrical material during the upsetting process.

In order to specifically study the effects of the boundary condition on the deformation of the alumina paste, the platens were lubricated with a silicone fluid in order to reduce the friction between the paste and the walls of the platens and to attempt to obtain a near perfect slip boundary condition. The appropriate friction coefficients for the unlubricated and lubricated interface conditions were found by comparing the experimental results with the FEA results so that the friction coefficients were in the best agreement between the predicted and experimental deformation patterns.

The effects of boundary condition on the deformation patterns of the alumina paste are illustrated in Fig. 8. A uniform flow pattern was obtained for the lubricated interface between the ceramic paste and the rigid walls of the platens [Fig. 8(b)]. Also, for the 'lubricated' interface condition, the folding and barrelling were almost absent.

Fig. 8(a) shows the experimental and predicted deformed configurations at ca 60% upsetting for the unlubricated interface condition. The maximum measured and predicted radius values, at 60% upsetting, which are about at the middle of the sample, are nearly identical for the 'unlubricated' upsetting test. The folding of the top and bottom outside surfaces of the billet onto the platens, as well as severe straining of the middle of the specimen, may be seen in Fig. 8(a). The chosen value of the Poisson's ratio, υ, has a strong influence upon the predicted flow patterns of the alumina

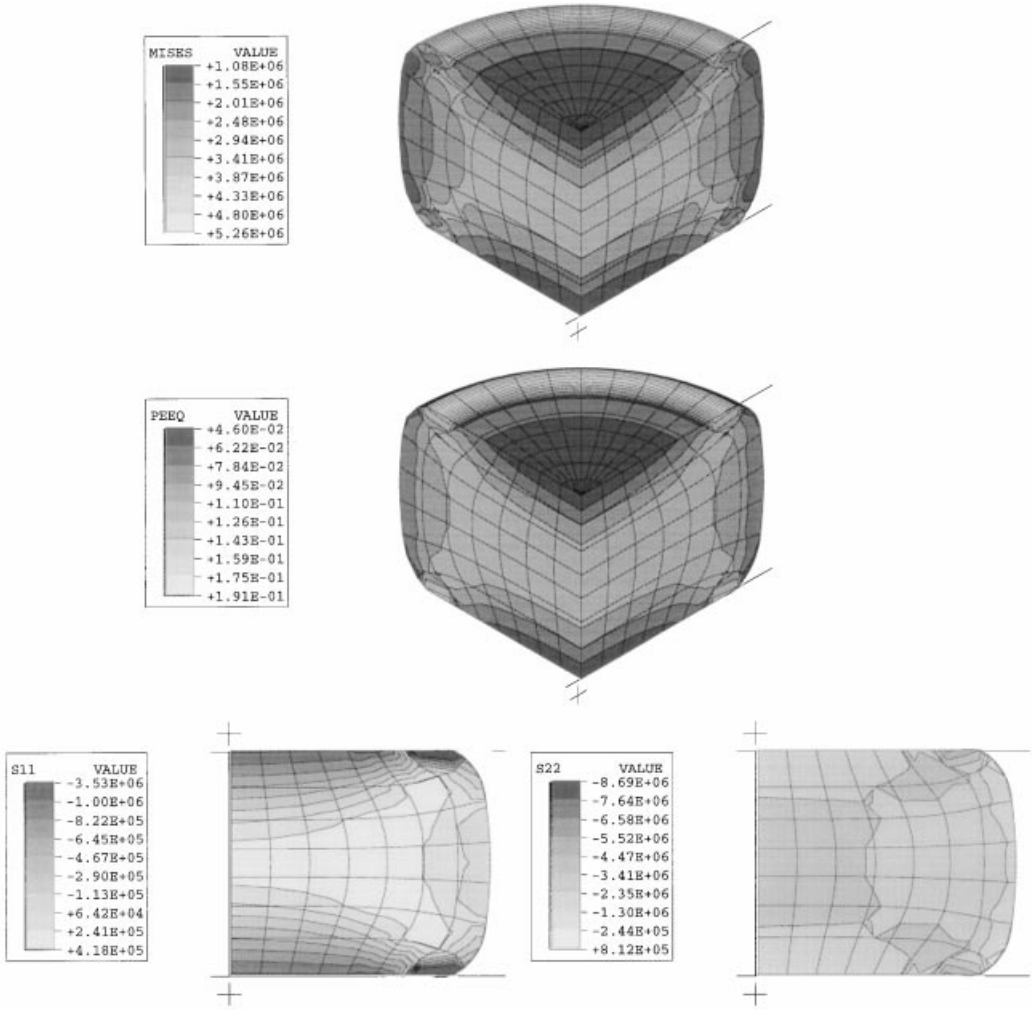

Fig. 7. The computed distributions of Mises stress, plastic equivalent strain, radial stress, and axial stress at 50% (nominal strain) upsetting for the 'unlubricated' interface boundary condition.

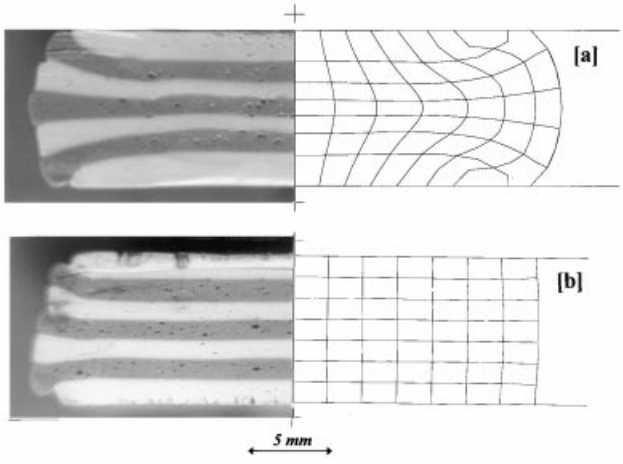

Fig. 8. The experimental and predicted deformed configurations for (a) 'unlubricated' platens, ca 60% (nominal strain) upsetting, and (b) 'lubricated' platens, ca 60% (nominal strain) upsetting.

paste. In order to obtain a good agreement between the predicted and experimental deformed patterns, the value of υ was selected as 0·33. Both the theoretical and experimental patterns remain quite symmetric about a horizontal line midway between the platens for the 'unlubricated' boundary condition. The predicted flow patterns agree remarkably well with the experimental results for the lubricated and unlubricated boundary conditions.

6 Conclusions

The rheological analysis of a ceramic paste was carried out using the squeeze film, upsetting and indentation hardness test configurations. The experimental results obtained for the upsetting configuration were compared with those found from the FEA analysis. A constitutive model, based upon an elasto-viscoplastic flow theory, was used for the FEA calculations. The material parameters for the ceramic paste, required for the FEA calculations, were measured using the squeeze film and indentation hardness test configurations. The simple first order analysis for the upsetting configuration cannot be used for the alumina paste system where the response is strongly dependent upon the imposed strain and the strain rates.

The calculations based upon the chosen response of 'a ceramic paste' show the potential for improving

the understanding of the flow behaviour of paste materials which may be applied to other processing techniques for 'soft solids'. The measured and predicted flow fields and applied force versus displacement curve, for this ceramic paste system, were found to be in good agreement. The evolution of internal structure during the deformation, including the 'folding' and 'barrelling' phenomenon, was predicted in detail. The flow patterns of the ceramic paste were strongly influenced by the interface condition between the ceramic paste and the walls of the plates.

The present analysis may also be used to examine those facets of the process which are difficult, if not impossible, to examine experimentally. The present finite element procedure may be implemented in order to model other types of tests on elasto-viscoplastic materials, such as extrusion and tape rolling and indeed the current indentation hardness and squeeze film configuration where first order explicit models have been used.

Finally, it has been shown that the necessary material parameters for the constitutive equations and FEA modelling may be obtained to a reasonable degree of accuracy using two simple experimental configurations; squeeze film and indentation hardness deformations.

Acknowledgements

The authors would like to acknowledge EPSRC for the financial support.

References

1. Kalyon, D. M., Yaras, P., Aral, B. and Yilmazer, U., Rheological behaviour of a concentrated suspension. *J. Rheo.*, 1993, **37**(1), 35.
2. Adams, M. J., Edmundson, B., Caughey, D. G. and Yayha, R., An experimental and theoretical study of the squeeze film deformation and flow of elastoplastic fluids. *J. Non-Newtonian Fluid Mech.*, 1994, **51**, 61.
3. Van Rooyen, G. T. and Backofen, W. A., Distributions of interface stresses in plane strain and axial symmetric compression. *Int. J. Mech. Physics of Solids*, 1957, **186**, 235.
4. Schey, J. A., Venner, T. R. and Takomana, S. L., Shape changes in the upsetting of slender cylinders. *J. Eng. Ind.*, 1982, **104**, 79.
5. Lin, Z. C. and Lin, S. Y., An investigation of a coupled analysis of a thermo-elastic-plastic model during warm upsetting. *Int. J. Mach. Tools Manufact.*, 1990, **30**, 599.
6. Adams, M. J., Aydin, I., Briscoe, B. J. and Sinha, S. K., A finite element analysis of the squeeze flow of an elasto-viscoplastic paste material. *J. Non-Newtonian Mechanics*, 1997, **71**, 41.
7. Özkan, N. and Briscoe, B. J., Preparation of ceria-gadolinia electrolytes by the tape rolling technique. *J. Mater. Res.*, 1998, **13**(3), 665.
8. Scott, J. P., Theory and application of the parallel plate plastometer. *Trans. Inst. Rubber Ind*, 1931, **40**, 481.
9. Sinha, S. K., Interface and bulk rheologies of soft solid pastes. PhD thesis, Imperial College, London, 1994.
10. Briscoe, B. J. and Sebastian, S., The elastic response of poly (methyl methacrylate) to indentation. *Proc. R. Soc. Lond. A*, 1996, **452**, 439.
11. Briscoe, B. J. and Özkan, N., Characterisation of ceramic pastes by an indentation hardness test. *J. Euro. Cer. Soc.*, 1997, **17**, 1675–1683.
12. Tabor, D., *Hardness of Metals*. Oxford University Press, UK, 1951.
13. Johnson, K. L., *Contact Mechanics*. Cambridge Press, Cambridge, 1985.
14. Bower, A. F., Fleck, N. A., Needleman, A. and Ogbonna, N., Indentation of a power law creeping solid. *Proc. R. Soc. Lond.*, 1993, **A441**, 97.